Hyperfine Interact (2016) 237:54
DOI 10.1007/s10751-016-1237-1

Mössbauer and X-ray study of biodegradation of $^{57}Fe_3O_4$ magnetic nanoparticles in rat brain

R. R. Gabbasov[1] · V. M. Cherepanov[1] · M. A. Chuev[1,2] · A. A. Lomov[2] · I. N. Mischenko[1,2] · M. P. Nikitin[3] · M. A. Polikarpov[1] · V. Y. Panchenko[1]

Abstract Biodegradation of a $^{57}Fe_3O_4$ - based dextran - stabilized ferrofluid in the ventricular cavities of the rat brain was studied by X-ray diffraction and Mössbauer spectroscopy. A two-step process of biodegradation, consisting of fast disintegration of the initial composite magnetic beads into separate superparamagnetic nanoparticles and subsequent slow dissolution of the nanoparticles has been found. Joint fitting of the couples of Mössbauer spectra measured at different temperatures in the formalism of multi-level relaxation model with one set of fitting parameters, allowed us to measure concentration of exogenous iron in the rat brain as a function of time after the injection of nanoparticles.

Keywords Mössbauer spectroscopy · X-ray diffraction · Superparamagnetic nanoparticles · Brain · Biodegradation

1 Introduction

Magnetic ferrofluids are increasingly used today in medicine for drug delivery, gene therapy, magnetic hyperthermia [1], contrasting of the magnetic - resonance images (MRI) [2] or 3D magnetic particle imaging (MPI) [3]. To implement all these procedures the ferrofluid, comprising magnetic nanoparticles, have to be introduced into the body either by direct

This article is part of the Topical Collection on *Proceedings of the International Conference on the Applications of the Mössbauer Effect (ICAME 2015), Hamburg, Germany, 13–18 September 2015*

✉ R. R. Gabbasov
graul@list.ru

[1] National Research Centre "Kurchatov Institute", Moscow, Russia

[2] Institute of Physics and Technology, Russian Academy of Sciences, Moscow, Russia

[3] Moscow Institute of Physics and Technology, Moscow, Russia

Published online: 22 February 2016

injections to the pathological organs or by intravenous injections with subsequent delivery by the blood stream into a target location. The ferrofluids, based on the iron oxide nanoparticles, are considered to be the most promising tools for such procedure. Their advantage is connected with the biocompatibility of iron. The human body contains several grams of endogenous iron, mainly in the form of ferritin or gem-containing proteins, such as the blood hemoglobin. Natural metabolism of iron in the body is a very intensive process. The iron released by the breakdown of hemoglobin or other iron-containing proteins, is reutilized repeatedly. The possibility of clearance of iron from a body is very limited, so the term "biodegradability" of magnetic nanoparticles usually means the transfer of the iron from the exogenous iron-containing nanoparticles into the endogenous iron-containing proteins, such as ferritin and hemoglobin. The iron absorption in humans is limited by a physiologic ceiling of about 3 mg/day. When the exogenous iron concentration exceeds the iron-binding capacity of transferrin, it appears in plasma as non-transferrin-plasma iron. The toxicity of non-transferrin-plasma iron is much higher than that of transferrin-iron [4]. Iron overload may result, for example, from transfusion therapy or increased dietary iron absorption [5, 6]. Therefore, development of methods to control biodegradation of iron oxide nanoparticles is of a great importance for introduction of magnetic nanoparticles based technologies into clinical practice.

Magnetic nanoparticles based technologies are very promising for the diagnostics and treatment of brain oncological or neurological disorders [7–11]. However, a specific feature of the brain, which is the presence of the blood–brain barrier, complicates processes of clearance of nanoparticles from the brain [12–15]. The purpose of the present work is to demonstrate applicability of Mössbauer spectroscopy to the quantitative evaluation of biodegradation of magnetic nanoparticles in the brain.

2 Experimental

2.1 Samples

The iron oxide based ferrofluid, enriched by the stable isotope ^{57}Fe, was prepared as previously reported [14, 15]. The intrinsic magnetic nanoparticles were synthesized with the sol-gel process by co-precipitation of $FeCl_2$ of the natural Fe isotope composition and $^{57}FeCl_3$ (Fe^{2+}: Fe^{3+} =1:2) with ammonia. The particles were magnetically washed with distilled H_2O and then coated with dextran. As a result, the produced magnetic nanoparticles were enriched with the ^{57}Fe stable isotope at the minimum of up to 66 %, which exceeds the ^{57}Fe content in magnetic nanoparticles of natural isotope composition in more than 30 times.

Details of the experiment on laboratory animals were described previously [16]. The right lateral ventricles of the brain of 17 Wistar rats were injected transcranially with 5 mL of ferrofluid containing 5 mg of magnetic $^{57}Fe_3O_4$ nanoparticles suspended in physiological saline. The injections were performed under chloral hydrate anesthesia. The animal care facility was kept under a natural light/dark cycle. The rats were housed individually and were provided with water and food ad libitum. The procedure was performed in compliance with the NIH guide for the care and use of laboratory animals (NIH Publication No. 8023, revised 1996). The rats were euthanized 15 min, 2 h, 1, 3, 7, 28, 49 and 84 days after the injection and the brains were extracted. For Mössbauer studies, the lyophilized rat brain samples were ground and the powder was alcohol precipitated onto a support made from polymethyl acrylate organic glass.

2.2 X-ray diffraction

SmartLab (Rigaku) diffractometer with a 9 kWt rotating anode was used for X-ray diffraction measurements of both initial magnetic nanoparticles (NP) and the brain, extracted 2 hours after the injection of these nanoparticles (2H), and also of the control brain (CB), extracted 2 hours after the injection of iron-free physiological saline solution. The measurements were carried out using $\theta - 2\theta$ scan in symmetric geometry and Cu K_α radiation. The incident parallel beam was created by a parabolically curved graded multilayer mirror. Reflection intensity was measured with 0.114 deg. soller slit and graphite flat crystal analyzer before a scintillation counter. To suppress the background on diffraction powder patterns specially cut single crystal silicon and glass (GH) sample holders for NP and 2H, CB were used respectively. X-ray diffraction patterns were collected by 2 s counting times per 0.05° step in the range of 20–80°.

2.3 Mössbauer spectroscopy

The Mössbauer absorption spectra of ^{57}Fe nuclei were measured in transmission geometry using an electrodynamical spectrometer working in the constant acceleration mode. ^{57}Co/(Rh) was used as the source of γ-radiation. Isomer shifts were determined relative to the absorption line of α-Fe.

3 Results and discussion

Figure 1 shows the X-ray diffraction patterns of the samples and glass holder GH. Phase identification for NP was done by using the ICDD database. It is clearly seen that the X-ray diffraction patterns do not contain a silicon reference line. Magnetite structure for magnetic nanoparticles NP pattern was evident. All diffraction peaks have symmetric broadening. This feature is a clear indication that the single-peak analysis is appropriate.

Evaluation of the lattice parameters and particles size was based on the fitting procedure from [17] by using the Voigt profile for diffraction peaks as shown in Fig. 2. The intensity of scattering from an ensemble of nanoparticles with the average diameter d is approximated by the Gaussian peaks with the widths [18]

$$\sigma_i = \frac{\lambda}{\sqrt{2\pi}\, d \cos\theta_{\mathrm{B}i}}, \tag{1}$$

where λis the wave length and θ_{Bi} is the Bragg angle corresponding to the i-th diffraction peak, which leads to the well known Scherrer formula for the FWHM value of the diffraction curve

$$\Delta\theta_i = 2\sqrt{2\ln 2}\,\sigma_i = \frac{0.94\lambda}{d\cos\theta_{\mathrm{B}i}}. \tag{2}$$

Taking into account the spectrometer resolution function, which in this case is determined mainly by the Lorentzian characteristic lines $K_{\alpha 1}$ and $K_{\alpha 2}$, the shape of each X-ray diffraction peak can be approximately described by the sum of two Voigt profiles with Gaussian width (1) and Lorentzian widths

$$\Gamma_{i,j} = \frac{\Delta\lambda_j}{\lambda}\left(\tan\theta_{\mathrm{B}i} - \tan\theta_{\mathrm{Bc}}\right), \tag{3}$$

where $\Delta\lambda_j$ ($j = 1{,}2$) are the widths of $K_{\alpha 1}$ and $K_{\alpha 2}$ lines and θ_{Bc} is the collimator Bragg angle. The fast procedure for numerical calculation of the required convolutions can be

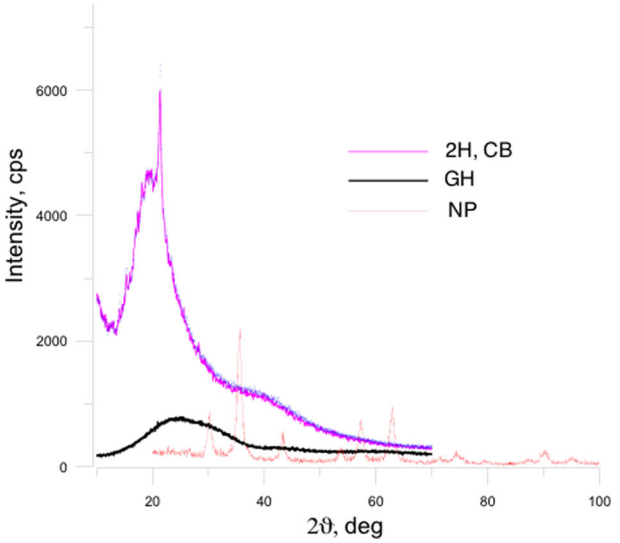

Fig. 1 X-ray diffraction powder patterns from the initial magnetic nanoparticles (NP) and from the brain extracted 2 hours after their injection (2H) as well as from the control brain without the nanoparticles (CB). GH is the glass holder, measured as reference

found in [17] and the results of such analysis for the most intensive peaks are presented in the Table 1.

The diffraction patterns of the bio-probes 2H and CB have a significantly different view in comparing with NP. The ratios of peak intensities for 2H and CB are practically equal, which points to a similar phase composition. The pattern has two extremely broad amorphous humps near at 20 and 40 deg. and a clearly visible sharp peak at 21.4 deg. which corresponds to interplanar distance d=0.414 nm. Nevertheless, there are still-detectable small peaks located in 15 - 20 deg. range. Angle positions of these peaks leads us to a conclusion, that all these features originate from bio-probe only and not from magnetite nanoparticles even for the sample 2H, which was prepared 2 hours after the injection. Failure in obtaining any information about magnetite particles is likely related to both more than ten times smaller concentration of them in bio-probes and remarkable scattering from amorphous phase of the glass sample holder.

Mössbauer spectra of ^{57}Fe in the dried ferrofluid and in the brain 2 hours, 1, 3 days, 4, 7 and 12 weeks after the injection, measured at 78 and 300 K, are shown in the Fig. 3. The Mössbauer spectrum of the initial ferrofluid at 300 K has the form of a sextet of highly asymmetric broadened lines. This form of the spectrum is not usual for superparamagnetic nanoparticles with the diameter of 10 nm (see Table 1) and can be explained only by the presence of dipole interparticle interaction in the sample [19–21]. Such behavior is typical for the spectra of ferrofluids consisting of so-called magnetic beads instead of individual magnetic nanoparticles. Each of the magnetic beads is composed from many magnetic nanoparticles fastened together by the polymeric shell. Within 2 hours after getting into a brain, the dextran shell begins to break down, and an additional central doublet of lines appears in the spectrum measured at 300 K. Generally, appearance of the doublet clearly indicates on biodegradation of the initial magnetic beads in the cerebrospinal fluid.

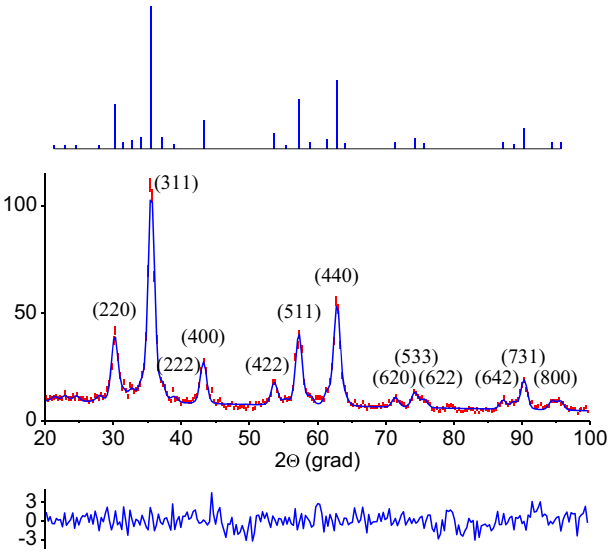

Fig. 2 Observed (*dashes*) and calculated (*line*) powder patterns from the magnetic nanoparticles together with their relative difference curve. *Upper dash* pattern presents data for magnetite Fe_3O_4 structure

Table 1 Average crystalline size of the initial magnetic nanoparticles evaluated from the X-ray diffraction peak widths

Peak	(311)	(440)
d, nm	10.2 (3)	10.2 (5)

On the other hand, this doublet may indicate both the appearance of the individual superparamagnetic nanoparticles in the brain, as a result of their release from the magnetically bound ensemble of the initial magnetic bead, and the generation of a new nonmagnetic iron-containing chemical compound as a result of the dissolution of the individual nanoparticles themselves.

The main idea of separation of the partial spectrum of these superparamagnetic nanoparticles from the partial spectrum of the paramagnetic compound is visible in Fig. 3. For example, the spectrum, measured at room temperature two hours after the injection, clearly shows a doublet. After lowering the temperature the doublet disappears almost completely and its intensity goes into a sextet. This indicates the superparamagnetic nature of the doublet. At twelve weeks we see the opposite behavior. The spectrum, measured at room temperature twelve weeks after the injection, clearly shows a doublet as well. But the lowering of the temperature does not affect the relative intensity of the doublet. Hence, some paramagnetic iron-containing chemical compound forms it. Thus, by lowering the measurement temperature, we can separate the components of the doublet.

To analyse the series of nanoparticles' Mössbauer spectra measured at different temperatures and on various stages of their biodegradation we proceeded from the well known multi-level approach [22] generalized on the case of existence on the resonance nuclei both magnetic dipolar and electric quadrupolar hyperfine interactions [23] and extended on ferrimagnetically-ordered materials exhibiting two magnetic sublattices. Hyperfine

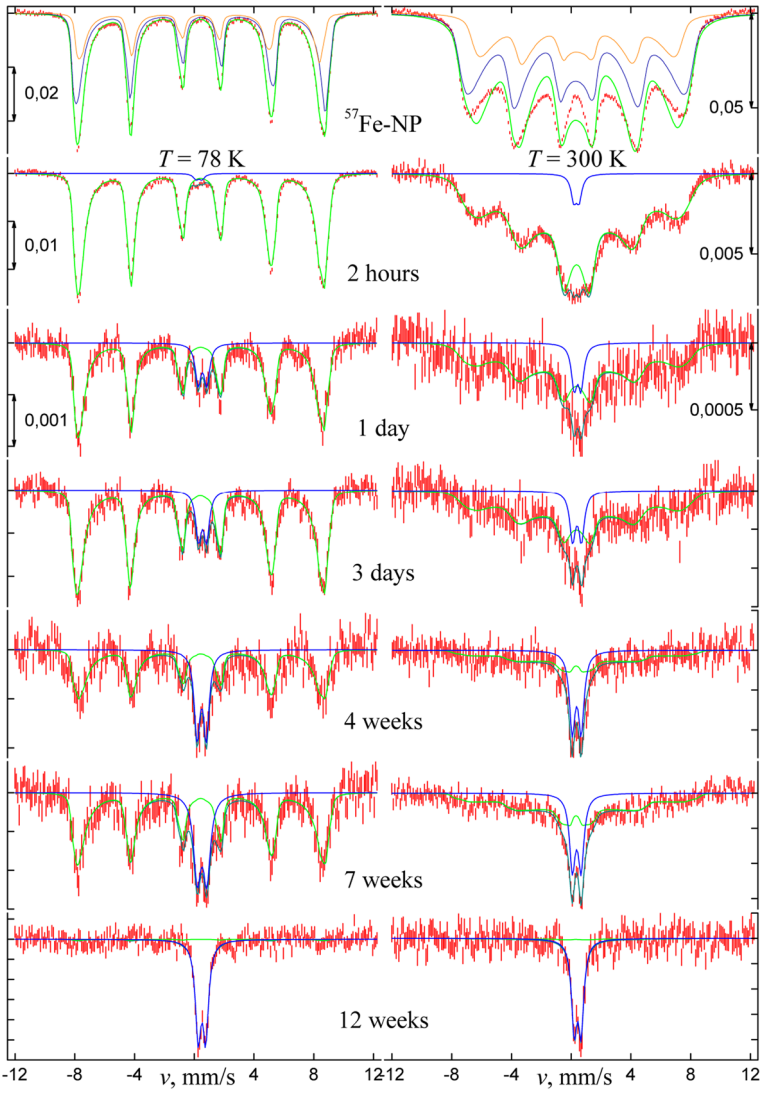

Fig. 3 ^{57}Fe Mössbauer spectra of the initial ferrofluid and of the rats brain 2 hours, 1, 3 days, 4, 7 and 12 weeks after its injection, measured at 78 and 300 K

parameters of isomer shift δ and quadrupolar splitting ΔEQ as well as intrinsic magnetic field H_{hf} in this representation are supposed to be individual for each of sublattices denoted as A and B, whereas magnetic and dynamical characteristics such as barrier height in the anisotropy field KV or diffusion constant for magnetization D as well as relative width of particles distribution over their diameters γ_d are considered as mutual for both sublattices. To describe the non-magnetic component of endogenous substance we chose standard pattern of broadened Lorentzian line split by quadrupolar interaction. To find the concentrations ^{57}n of ^{57}Fe in the endogenous and exogenous phases, the Debye model of solid body structure was used.

Table 2 Mössbauer parameters, corresponding to the spectra of the initial ferrofluid and the rats brain 2 hours, 1, 3 days, 4, 7 and 12 weeks after its injection, shown in Fig. 3: $\delta_{A,B,p}$ – isomer shift, $\Delta EQ_{A,B,p}$ – quadrupolar splitting, $H_{hf\,A,B}$ – hyperfine field, Γ_p – line width for the ferrimagnetic sublattices A and B and paramagnetic component p, D – diffusion constant, KV – anisotropy energy, γ_d – relative width of Gaussian distribution of nanoparticles over their diameters, ^{57}n and $^{57}n_p$ – ^{57}Fe concentrations in the superparamagnetic nanoparticles and in the nonmagnetic iron-containing chemical compound

	NP / Rats		2 hours		1 day		3 days		4 weeks		7 weeks		12 weeks	
T,K	78	300	78	300	78	300	78	300	78	300	78	300	78	300
Superparamagnetic component														
γ_d	0.30 (1)		0.38 (4)		0.4		0.4		0.4		0.4		0.4	
KV, K	420 (10)	390 (10)	410 (50)	80 (10)	350 (40)	90 (30)	310 (30)	80 (30)	230 (40)	40 (30)	230(30)	30(20)	230	30
D, mm/s	0	1.05 (1)	0	0.11 (2)	0	0.1 (1)	0	0.1 (1)	0	0	0	0	0	0
ΔEQ_A, mm/s	0.70 (1)		0.70 (1)		0.70 (5)		0.70 (5)		0.7 (1)		0.7 (1)		0.7	
ΔEQ_B, mm/s	0.72 (1)		0.72 (2)		0.72 (10)		0.72 (9)		0.7 (3)		0.7 (2)		0.7	
$H_{hf\,A}$, kOe	523.8 (1)	513 (1)	519.8 (2)	510 (5)	519 (1)	510 (30)	524 (1)	510 (30)	525 (3)	510 (30)	526 (2)	510 (10)	526	510
$H_{hf\,B}$, kOe	505.0 (3)	461 (1)	500.9 (6)	460 (10)	501 (3)	460 (50)	506 (2)	460 (50)	500 (6)	460 (60)	508 (5)	460 (20)	508	460
δ_A, mm/s	0.460 (1)	0.33 (1)	0.466 (2)	0.33 (2)	0.47 (1)	0.3 (1)	0.43 (1)	0.3 (1)	0.45 (3)	0.3 (3)	0.45 (2)	0.3 (1)	0.45	0.3
δ_B, mm/s	0.379 (3)	0.40 (1)	0.386 (4)	0.40 (4)	0.36 (2)	0.4 (2)	0.39 (2)	0.4 (2)	0.46 (5)	0.4 (5)	0.43 (4)	0.4 (2)	0.43	0.4
^{57}n, 10^{16}cm^{-3}	10(4)*e5		390* (70)		23* (3)		27* (3)		16 (1)		26 (1)		1 (1)	
Paramagnetic component														
ΔEQ_p, mm/s		0.69 (12)	0.41 (6)	0.36 (4)	0.58 (4)	0.47 (7)	0.54 (3)	0.60 (5)	0.61 (3)	0.60 (3)	0.64 (3)	0.59 (2)	0.50 (1)	0.45 (2)
δ_p, mm/s		0.37 (10)	0.32 (4)	0.35 (2)	0.55 (2)	0.43 (4)	0.56 (2)	0.39 (3)	0.50 (2)	0.37 (1)	0.52 (2)	0.37 (1)	0.52 (1)	0.43 (1)
Γ_p, mm/s		0.45 (7)	0.45 (12)	0.45 (9)	0.45 (6)	0.45 (13)	0.45 (5)	0.45 (9)	0.45 (4)	0.45 (4)	0.58 (5)	0.46 (3)	0.45 (2)	0.44 (4)
$^{57}n_p$, 10^{16}cm^{-3}	3.7* (7)		4.3* (4)		2.6* (2)		3.5* (3)		7.1* (13)		9.0* (2)		15.7 (4)	

* Values were calculated using averaging over times of 1 day and more

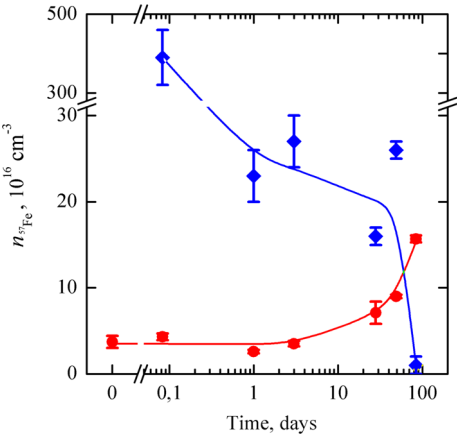

Fig. 4 Dependence of ^{57}Fe-isotope concentration retained in the rats brain in the form of superparamagnetic nanoparticles (*diamonds*) and paramagnetic iron-containing chemical compound (*circles*) on the time of magnetic beads biodegradation. *Lines* are guides to the eye

Resulting and partial superparamagnetic and nonmagnetic spectra are shown in Fig. 3 by thick lines. Thin lines on the graphs for initial ferrofluid describe two magnetic sublattices. Table 2 represents corresponding physical parameters, which characterize changes of the magnetic beads in the process of their biodegradation. These data were obtained by simultaneous analysis of the couples of Mössbauer spectra measured at 78 and 300 K. It is interesting to note that the anisotropy energy of the magnetic nanoparticles decreases monotonically with the time after the ferrofluid injection into a living organism. This is an additional evidence in favour of our assumption about the presence of magnetically coupled superparamagnetic particles in the initial beads. Curves in Fig. 4 show changes of the ^{57}Fe concentration both in superparamagnetic nanoparticles and paramagnetic iron-containing chemical compound in the brain with the time after the injection.

Control spectra of the ^{57}Fe in the brain of the rats 2 hours, 1 and 3 days after the injection of iron-free physiological saline solution, measured at room temperature, are shown in Fig. 5. They demonstrate only a small doublet of lines, related to endogenous iron-containing paramagnetic compound. Table 3 represents parameters of the spectra. Fit of the spectra with these parameters allowed us to estimate the concentration of endogenous ^{57}Fe in the brain of the control rats, which is presented in the last line of the Table 3. It is seen that the concentration of ^{57}Fe in the form of the paramagnetic iron-containing chemical compound detected in the brain of the rats 2 hours, 1 and 3 days after the injection of the ^{57}Fe - enriched ferrofluid (see Fig. 4), is comparable with the concentration of endogenous ^{57}Fe in the brain of the control rats. We can therefore conclude that the generation of this endogen-like nonmagnetic iron-containing chemical compound from the exogenous magnetite nanoparticles started only since the third day after the injection. Up to this point, only the decomposition of the initial magnetic beads onto the superparamagnetic magnetite nanoparticles is evident.

It is worth mentioning that X-ray diffraction patterns for magnetite and maghemite nanoparticles differ only slightly and the question on the phase composition in the studied samples is usually solved with involving Mössbauer data. The bulk materials spectrum of Fe_3O_4 is distinguished from one of γ-Fe_2O_3 by the presence of the magnetic sextet corresponding to Fe^{2+} ions. Besides, bulk magnetite exhibits Verwey phase transition at about 120 K, so that its Mössbauer spectra change dramatically when going through this point (see, for example, [32]). For nanosize samples situation is not so unambiguous in respect to both the ability to distinguish among magnetite and maghemite as well as the presence of

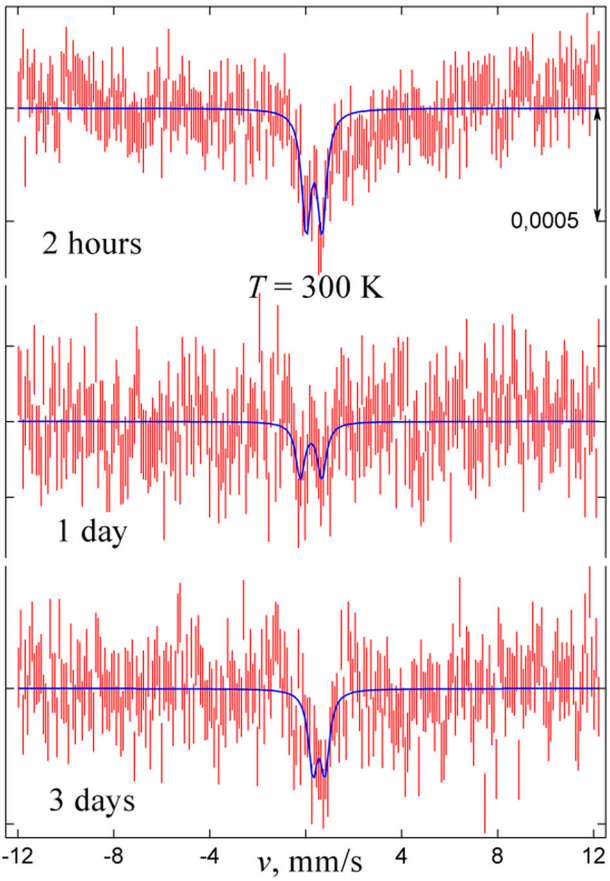

Fig. 5 ^{57}Fe Mössbauer spectra of the brain of the control rats 2 hours, 1 and 3 days after the injection of iron-free physiological saline solution, measured at 300 K

Table 3 Mössbauer parameters, corresponding to the spectra of the brain of the control rats 2 hours, 1 and 3 days after the injection of iron-free physiological saline solution, shown in Fig. 5: ΔEQ_p – quadrupolar splitting, δ_p – isomer shift, Γ_p – full width of the line, $^{57}n_p$ – endogenous ^{57}Fe-isotope concentration, found in the brain in the form of paramagnetic iron-containing compound

Time	2 hours	1day	3 days	Average
ΔEQ_p, mm/s	0.66 (5)	0.90 (14)	0.50 (8)	0.69 (12)
δ_p, mm/s	0.35 (3)	0.22 (8)	0.55 (5)	0.37 (10)
Γ_p, mm/s	0.45 (7)	0.45 (19)	0.45 (14)	0.45 (7)
$^{57}n_p$, 10^{16}cm^{-3}	5.1 (5)	3.2 (7)	2.7 (4)	3.7 (7)

Verwey transition itself. One of the probable ways to explain such behavior was proposed in [32].

To clarify phase composition of the samples experimentally we measured Mössbauer spectra of the dried ferrofluid and biological probes in a magnetic field strong enough for

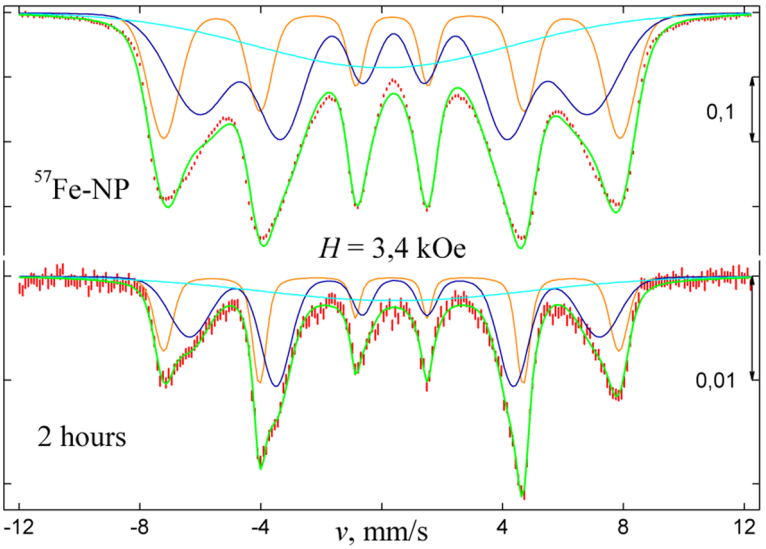

Fig. 6 ^{57}Fe Mössbauer spectra of the initial ferrofluid and the rat brain 2 hours after its injection, measured at 300 K in the transversal magnetic field of 3.4 kOe

Table 4 Mössbauer parameters, corresponding to the spectra of the initial ferrofluid and the rat brain 2 hours after its injection, measured in the magnetic field and shown in Fig. 6: S – relative spectral area of the component, H_{hf} – hyperfine field, δ – isomer shift, QS – quadrupolar shift, σ_1 and σ_3 – Gaussian broadening of the outer and inner pairs of Mössbauer lines, respectively, and I_2 / I_3 – ratio of intensities of the intermediate and inner pairs of lines

	Parameter	S, %	H_{hf}, kOe	δ, mm/s	QS, mm/s	σ_1, mm/s	σ_3, mm/s	I_2 / I_3
NP	Sublattice A	48 (1)	400 (1)	0.40 (1)	0.00 (1)	0.97 (1)	0.42 (1)	2.7 (1)
	Sublattice B	28 (1)	469 (1)	0.34 (1)	0.00 (1)	0.45 (1)	0.21 (1)	1.8 (1)
	Singlet	24 (1)	–	0.05 (1)	–	4.2 (1)	–	–
2 hours	Sublattice A	49 (2)	422 (2)	0.43 (1)	0.00 (3)	0.60 (3)	0.26 (2)	4.2 (4)
	Sublattice B	28 (2)	468 (1)	0.32 (1)	0.00 (1)	0.24 (1)	0.08 (2)	3.4 (4)
	Singlet	23 (4)	–	0.4 (1)	–	4.4 (5)	–	–

the nearly full remagnetization of the system (see Fig. 6). It is clearly seen even from visual inspection that the spectra exhibit two nonequivalent magnetic sextets, which qualitatively correspond to the spectral shape of magnetite. Decomposition of the experimental curves on two magnetic and an additional distributed component (see Table 4) only corroborates this impression, revealing different chemical shifts of the sublattices as an evidence of various electronic environments of the resonant nuclei. Moreover, quadrupolar interaction seems to play no essential role upon this decomposition, what is usually considered as an argument for the structure of magnetite. Specific variations of the hyperfine parameters in small particles lead to a visible broadening of the resonant lines, and so to describe it we introduced normal distribution function and calculated resulting shape of the Mössbauer peaks by means of numerical procedure from [17]. Nevertheless, to the present day there is no consistent theory of ferrimagnetic nanoparticles in the field, so we have been forced

to restrict ourselves by such a formal analysis and have not been able to realize previously proposed more reliable analytical technique for diagnostics of magnetic nanoparticles in a living organism [33]. The work in this direction is continuing.

4 Conclusions

The study showed that in rat brain there is a two-stage process of biodegradation of the magnetite based ferrofluid. The first step is the decomposition of initial aggregative magnetic beads onto the superparamagnetic magnetite nanoparticles and the second step is the generation of a new paramagnetic iron-containing chemical compound from the magnetite nanoparticles. Many possible forms of endogenous iron in the brain tissue, including heme iron, different forms of ferritin and hemosiderine, magnetite, maghemite and even wustite are reported [24–31], which have similar Mössbauer parameters. Identification of the paramagnetic compound detected in this study, is beyond the scope of this article and requires research methods, more sensitive to small concentrations of these substances.

Acknowledgments The work on the synthesis of isotopically enriched nanoparticles was supported in part by the Russian Science Foundation under Grant 14-15-01096. The theoretical study of dipole interactions in ensembles of magnetic nanoparticles was supported in part by the Russian Foundation for Basic Research under Grant 14-29-10226. The work on the study of biodegradation in vivo was supported in part by the Russian Foundation for Basic Research under Grant 13-02-12462.

References

1. Pankhurst, Q.A., et al: Progress in applications of magnetic nanoparticles in biomedicine. J. Phys. D: Appl. Phys. **42**, 224001 (2009)
2. Krishnan, K.M.: Biomedical nanomagnetics: a spin through possibilities in imaging, diagnostics, and therapy. IEEE Trans. Magn **46**, 2523–2558 (2010)
3. Gleich, B., Weizenecker, J.: Tomographic imaging using the nonlinear response of magnetic particles. Nature **435**, 1214–12147 (2005)
4. Hershko, C., Link, G., Cabantchik, I.: Pathophysiology of iron overload. Ann. N.Y. Acad. Sci. **850**, 191–201 (1998)
5. St. Pierre, T.G., et al.: Multicenter validation of spin-density projection-assisted r2-MRI for the noninvasive measurement of liver iron concentration. Magn. Reson. Med. **71**, 2215–2223 (2014)
6. St. Pierre, T.G., et al.: Iron overload diseases: the chemical speciation of non-heme iron deposits in iron loaded mammalian tissues. Hyperfine Interact. **126**, 75–81 (2000)
7. Chertok, B.A., Moffat, A.E., et al.: Iron oxide nanoparticles as a drug delivery vehicle for MRI monitored magnetic targeting of brain tumors. Bio- materials **29**(4), 487–496 (2008)
8. Zainulabedin, M.S., Nimisha, H.G., Madhavan, P.N.: Magnetic nanoformulation of azidothymidine 5-triphosphate for targeted delivery across the blood–brain barrier. Int. J. Nanomed. **5**, 157–166 (2010)
9. Riviere, C., Martina, M.S., Riviere, C., et al.: Magneting targeting of nanometric magnetic fluid loaded liposomes to specific brain intravascular areas: a dynamic imaging study in mice. Radiology **244**, 439–448 (2007)
10. Jain, S., Mishra, V., Singh, P., Dubey, P.K., Saraf, D.K., Vyas, S.P.: RGD-Anchored magnetic liposomes for monocytes/neutrophils-mediated brain targeting. Int. J. Pharm. **261**, 43–55 (2003)
11. Liu, et al.: Magnetic resonance monitoring of focused ultrasound/magnetic nanoparticle targeting delivery of therapeutic agents to the brain. Proc. Natl. Acad. Sci **107**(34), 15205–15210 (2010)
12. Polikarpov, D.M., Gabbasov, R.R., Cherepanov, V.M., Chuev, M.A., Korshunov, V.A., Nikitin, M.P., Deyev, S.M., Panchenko, V.Y.: Biodegradation of magnetic nanoparticles in rat brain studied by Mössbauer spectroscopy. IEEE Trans. Magn. **49**, 436–439 (2013)
13. Polikarpov, D.M., Cherepanov, V.M., Gabbasov, R.R., Chuev, M.A., Mischenko, I.N., Korshunov, V.A., Panchenko, V.Y.: Efficiency analysis of clearance of two types of exogenous iron from the rat brain by Mössbauer spectroscopy. Hyperfine Interact. **218**(1–3), 83–88 (2013)

14. Polikarpov, D., Cherepanov, V., Chuev, M., Gabbasov, R., Mischenko, I., Nikitin, M., Vereshagin, Y., Yurenia, A., Panchenko, V.: Mössbauer evidence of $^{57}Fe_3O_4$based ferrofluid biodegradation in the brain. Hyperfine Interact. **226**, 421–430 (2014)
15. Nikitin, M.P., Shipunova, V.O., Deyev, S.M., Nikitin, P.I.: Biocomputing based on particle disassembly. Nat. Nanotechnol. **9**(9), 716–722 (2014)
16. Polikarpov, D., Gabbasov, R., Cherepanov, V., Loginova, N., Loseva, E., Nikitin, M., Yurenia, A., Panchenko, V.: Mössbauer study of exogenous iron redistribution between the brain and the liver after administration of $^{57}Fe_3O_4$ferrofluid in the ventricle of the rat brain. J. Magn. Magn. Mater. **380**, 78–84 (2015)
17. Chuev, M.A.: An efficient method of analysis of the hyperfine structure of gamma-resonance spectra using the Voigt profile. Doklady Phys. **56**(6), 318–322 (2011)
18. Zachariasen, W.H.: Theory of X-ray Diffraction in Crystals. Willey, New York (1945)
19. Polikarpov, M., Trushin, I., Yakimov, S.: Temperature relaxation of a superferromagnetic state in dispersed hematite. J. Magn. Magn. Mater. **116**, 372 (1992)
20. Mørup, S., Hansen, M.F., Frandsen, C.: Magnetic interactions between nanoparticles. Beilstein J. Nanotechnol. **1**, 182–190 (2010)
21. Gabbasov, R.R., Polikarpov, M.A., Cherepanov, V.M., Chuev, M.A., Panchenko, V.Y.: Breaking of interparticle interaction in conjugates of magnetic nanoparticles injected into the mice. Hyperfine Interact. **206**, 71–74 (2012)
22. Jones, D.H., Srivastava, K.K.P.: Many-state relaxation model for the Mössbauer spectra of superparamagnets. Phys. Rev. B **34**, 7542–7548 (1986)
23. Chuev, M.A.: Multi-level relaxation model for describing the Mössbauer spectra of single-domain particles in the presence of quadrupolar hyperfine interaction. J. Phys.: Condens. Matter **23**, 426003 (11pp) (2011)
24. Pankhurst, Q., Hautot, D., Khan, N., Dobson, J.: Increased levels of magnetic iron compounds in Alzheimer's disease. J. Alzheimers Dis. **13**(1), 49–52 (2009)
25. Kirschvink, J.L., Kobayashi-Kirschvink, A., Woodford, B.J.: Magnetite biomineralization in the human brain. Proc. Nat. Acad. Sci. **89**, 7683–7687 (1992)
26. Dunn, J.R., Fuller, M., Zoeger, J., Dobson, J., Heller, F., Hammann, J., Caine, E., Moskowitz, B.M.: Magnetic material in the human hippocampus. Brain Res. Bull. **36**, 149–153 (1995)
27. Dobson, J., Grassi, P.: Magnetic properties of human hippocampal tissue: Evaluation of artefact and contamination sources. Brain Res. Bull. **39**, 255–259 (1996)
28. Quintana, C., Lancin, M., Marchic, C., Pérez, M., Martin-Benito, J., Avila, J., Carrascosa, J.L.: Initial studies with high resolution TEM and electron energy loss spectroscopy studies of ferritin cores extracted from brains of patients with progressive supranuclear palsy and Alzheimer disease. Cell Mol. Biol. **46**, 807–820 (2000)
29. Quintana, C., Cowley, J.M., Marhic, C.: Electron nanodiffraction and high-resolution electron microscopy studies of the structural and composition of physiological and pathological ferritin. J. Struct. Biol. **147**, 166–178 (2004)
30. Hautot, D., Pankhurst, Q.A., Khan, N., Dobson, J.: Preliminary evaluation of nanoscale biogenic magnetite in Alzheimer's disease brain tissue. Proc. R. Soc. Lond. Ser. B **270**, S62–S64 (2003)
31. Brem, F., Hirt, A.M., Winkelhofer, M., Frei, K., Yonekawa, Y., Wieser, H.G., Dobson, J.: Magnetic iron compounds in the human brain: A comparison of tumour and hippocampal tissue. J. R. Soc. Interface **3**(11), 833–841 (2006)
32. Chuev, M.A.: On the shape of gamma-resonance spectra of ferrimagnetic nanoparticles under conditions of metamagnetism. JETP Lett. **98**(8), 465–470 (2013)
33. Mischenko, I., et al.: Biodegradation of magnetic nanoparticles evaluated from Mössbauer and magnetization measurements. Hyperfine Interact. **219**, 57–61 (2013)